Heliyon 11 (2025) e43454

Contents lists available at ScienceDirect

Heliyon

journal homepage: www.cell.com/heliyon

Research article

Spatiotemporal assessment of land use land cover dynamics in Mödling district, Austria, using remote sensing techniques

Gbenga Lawrence Alawode [a], Tomiwa Victor Oluwajuwon [b], Rasheed Akinleye Hammed [a,*], Kehinde Ezekiel Olasuyi [c], Andrey Krasovskiy [d], Oluwadamilola Christianah Ogundipe [e], Florian Kraxner [d]

[a] Faculty of Science, Forestry and Technology, University of Eastern Finland, 80101, Joensuu, Finland
[b] Tropical Forests and People Research Centre, University of the Sunshine Coast, Sippy Downs, QLD, 4556, Australia
[c] Department for Innovation in Biological, Agro-food and Forest Systems, University of Tuscia, Viterbo, 01110, Italy
[d] Agriculture, Forestry and Ecosystem Services Group, Biodiversity and Natural Resources Program, International Institute of Applied Systems Analysis, Schlossplatz 1, A-2361, Laxenburg, Austria
[e] Swiss Federal Research Institute, WSL Zürcherstrasse 111, CH-8903, Birmensdorf, Switzerland

ARTICLE INFO

Keywords:
Change detection
CORINE
Landsat
Remote sensing
Settlement
Vegetation index

ABSTRACT

Remotely sensed imagery plays a crucial role in analyzing and monitoring land cover and urban growth. The accuracy and applicability of European CORINE Land Cover (CLC) maps in Land Use and Land Cover (LULC) monitoring across European regions, especially at local scales, have been critiqued and remain limited due to temporal methodological variations. This study aims to understand the dynamics of LULC, assess the effectiveness of vegetation indices in estimating forest cover, and validate the local applicability of CORINE maps in the Lower Austrian district of Mödling in the neighbourhood of Vienna from 1999 to 2022. We employed a supervised maximum likelihood classifier and class-based change detection to analyze multi-decadal multispectral imagery for mapping and quantifying vegetation and land use changes across the district, in comparison with satellite indices and CORINE data. The study identified changing patterns and assessed the accuracy of the Normalized Difference Vegetation Index (NDVI) and the Soil Adjusted Vegetation Index (SAVI) in estimating Mödling's forest cover, determining optimal thresholds for improved assessment. Our findings reveal a slight reduction in Mödling's forest area – decreasing from 39.11 % in 1999 to 36.5 % in 2022 – with an overall reduction of 2.61 %. Agriculture primarily caused forest loss in the early period, expanding by over 37 %. In the most recent decade, settlement expansion, with built-up areas gaining approximately 650 ha, has exacerbated the loss of forest and agricultural lands. Our classification achieved high overall accuracy (92 %–94 %) and Kappa accuracy (0.90–0.93). The supervised classification exhibited a consistent reduction, aligning with CORINE outputs and refuting reports of its limited local applicability and accuracy. Although NDVI and SAVI estimates revealed a non-monotonic trend in forest cover across different years, NDVI performed better than SAVI. The results of this study are vital, providing evidence and recommending effective measures for enhancing monitoring, policy development, and decision-making regarding vegetation conservation, urban development, and overall land management. This research contributes to the limited body of core studies employing spectral imagery and GIS tools to monitor changes in land cover or assess CORINE maps in Austria and across Europe, with a special focus on the peri-urban interface.

* Corresponding author.
E-mail address: hammedrasheedakinleye@gmail.com (R.A. Hammed).

https://doi.org/10.1016/j.heliyon.2025.e43454
Received 30 January 2024; Received in revised form 23 May 2025; Accepted 26 May 2025

1. Introduction

The use of remote sensing data has become indispensable for analyzing the dynamics of land cover [1,2]. Satellite imagery has gained widespread recognition in global research projects, particularly in the domains of climate change, ecological monitoring, and environmental research [3–6]. In recent times, change detection methodologies employing Geographic Information System (GIS) tools and remote sensing (RS) data for image processing and classification have been given significant attention [7–9]. Hence, these approaches (GIS and RS) prove to be well-suited for identifying changes in land use and land cover patterns [10–12].

Global population growth, settlement expansion, industrialization, and climate change impacts have resulted in unforeseen shifts in Land Use and Land Cover (LULC) dynamics, and resilient land use management and monitoring measures are more important than ever before [13]. To this end, the significance of LULC mapping and analysis, coupled with the regular monitoring of dynamic changes, cannot be overstated. This underscores the imperativeness of utilizing suitable remote sensing-based data alongside effective change detection approaches [5,14]. Of utmost importance, gathering, classifying, validating, and storing change-related data requires consideration of many factors and methods that have garnered increasing prominence in recent times [3,15,16]. This widespread recognition is due to RS data being collected and stored in a digital format, which facilitates subsequent operations on computers and supports modelling approaches [2,17,18]. Remote sensing technologies provide extended spatial coverage and multispectral data, ensuring a consistent supply of reliable and precise information [2,17].

Over the years, researchers worldwide have published and presented several scientific studies focusing on the use of satellite imagery with varying resolutions to detect changes in land-use patterns [2,12,19–21]. Satellite imagery – including Landsat data, Sentinel data, and other data sources – has become crucial for conducting effective analysis, mapping, accounting, and monitoring of LULC changes on local, national, and global scales [16,22–24]. Despite the suitability of remotely sensed data for detecting and analyzing LULC changes across different spatial and temporal scales within the Austrian context, limited attention has been given to municipal-level analysis [25,26]. To the best of the authors' knowledge, no research has been conducted to analyze land-use changes in Mödling, a significant district in Lower Austria currently undergoing landscape transformation. Such a study would be instrumental in predicting the progression of future vegetation cover, especially in light of anticipated LULC transformations within the region. Consequently, LULC change detection studies are essential for helping the government and land managers at the local level implement improved land use management policies and provide appropriate strategies for maintaining various natural environments.

Vegetation indices (VIs) derived from geospatial data obtained from sensors have become vital tools for researchers all over the world [27–29]. VIs are widely utilized for analyzing the characteristics of vegetation and forest structures [28,30,31]. The effectiveness of these indices has been demonstrated in studies which have shown their ability to provide relatively precise estimations of multispectral imaging [32–34]. In addition, they are critical for scientists studying the complexities of vegetative dynamics and their responses to environmental changes [32,35]. Among the VIs available, the Normalized Difference Vegetation Index (NDVI) and Soil Adjusted Vegetation Index (SAVI) have been extensively used in various RS applications [32,35–37]. Normalized Difference Vegetation Index and Soil Adjusted Vegetation Index are calculated based on the differences in reflectance between the near-infrared (NIR) and RED bands. These provide an integral metric for assessing vegetation density and tracking its temporal growth [38,39]. Normalized Difference Vegetation Index stands out as the most important and popular index for vegetation assessment, mainly because of its ability to distinguish between vegetative and non-vegetative entities such as soil or water and detect even minor vegetation changes [40,41]. However, despite its strength, NDVI has drawbacks, which include its inability to accurately predict changes in soil colour and soil water content, and its susceptibility to saturation from densely vegetated areas [39,42]. To address these limitations, the adoption of SAVI has become crucial and is garnering increasing attention in RS studies. Soil Adjusted Vegetation Index is an effective algorithm that is more suitable for analyzing vegetation in areas with bare soil or high soil reflectance [39,43,44]. Therefore, the combined use of NDVI and SAVI has revolutionized how researchers obtain more detailed and accurate information about vegetation and soil conditions, making these algorithms essential tools for climate change, ecological, and GIS/RS studies [32]. Consequently, it is important to better understand their limitations and capabilities to maximize the effectiveness and application of these spectral indices, as studies have demonstrated variability in their accuracy and suitability for assessing certain LULC classes [45,46]. This knowledge will aid researchers in accurately monitoring vegetation growth patterns, assessing forest health conditions, and tracking the effects of climate change on vegetation ecosystems.

CORINE Land Cover (CLC) maps are standardized periodic maps developed for monitoring and analyzing changes in LULC across diverse European regions [47–50]. These maps are valuable for researchers and policymakers and have become essential tools for numerous purposes, including environmental monitoring, natural resource management, and land-use planning [50]. However, despite their considerable benefits, the use of these maps has been limited, especially at the local level, such as in Mödling, Lower Austria. Therefore, it is imperative to integrate these mapping methodologies to better understand and monitor changes in LULC dynamics, which can aid in developing robust land management strategies [51,52]. Nevertheless, the accuracy of available European CLC maps in monitoring land-use changes tends to vary with the geographical complexity and land cover heterogeneity of the specific country to which they are applied [49]. Studies have highlighted uncertainties, inaccuracies, and limitations in the applicability of the maps in specific national cases like Spain and the Netherlands [47,51], but no known case study exists for Austria. Furthermore, existing studies have evaluated accuracy by comparing new CORINE maps with previous editions, a method that might not be the most effective approach for validation. A more suitable approach involves using unique land cover products and dynamic LULC maps on the same geographical or territorial extent, an approach that is scarce in the region, except for the study conducted across the European Alps using a low-resolution MODIS-based land cover comparative analysis [53]. Additionally, the variability in CORINE accuracy is exacerbated by methodological variations in the temporal production of the CORINE maps. Since its initiation in 1990, CORINE has been updated every six years, experiencing changes in methodologies from photo interpretation techniques to the generalization approach of individual national maps [47,52]. This phenomenon is argued to pose limitations on their usability for long-term LULC change analysis, albeit with limited justification.

This study aimed to examine LULC dynamics in the Mödling district, Lower Austria, from 1999 to 2022 using Landsat multispectral imagery. The study objectives are: (a) to understand the land cover dynamics of Mödling using a supervised classification algorithm, (b) to explore the suitability and accuracy of vegetation spectral indices in estimating forest cover in the study area, and (c) to conduct a two-way validation between the CORINE Land Cover maps and our supervised classification outputs to enhance the overall precision and confidence in land cover information derived from both methodologies.

2. Methods

2.1. Study area

Mödling is one of the 20 districts in Lower Austria, situated between latitudes 47°57'30"N and 48°13'9"N and longitudes 16°3'30"E and 16°33'21"E (Fig. 1). It is located adjacent to southern Vienna in the “Industriviertel” (industrial area) of Lower Austria. Lower Austria (Niederosterreich) is in the northeastern part of Austria and is one of the nine states in the country. It is one of the largest states, covering an area of 19,186 km2, and shares international borders with the Czech Republic in the South Bohemia and South Moravia regions, as well as Slovakia in the Bratislava and Tmava regions. The state is divided into four regions, often referred to as Vierta: Weinveirtel (wine quarter), Waldviertel (forest quarter), Mostviertel (most quarter), and Industrieviertel (industrial quarter). The industrial quarter comprises seven districts, one of which is Mödling. Geographically, the district of Mödling has a total population of 121,039 inhabitants [54]. It experiences a temperate climate typical of Central Europe, characterized by four distinct seasons, including cold winters and warm summer periods. The climate in this region is of a Pannonic sub-continental type, with annual precipitation and temperature averaging around 650–800 mm and 7–10 °C, respectively [55–57]. The Lower Austria region encompasses various soil types, primarily consisting of Cambisols, Planosols, and Kolluvisols [57]. It contains several water bodies and watersheds that serve as essential habitats for biodiversity, including Mödlinger Bach, Schwechat River, and Wienerwald lakes, among others [57,58]. The vegetation in the Mödling district is characterized by a diverse mixture of forests, meadows, agricultural and grassland areas, as well as urban settlements. The forested areas in this district are home to various tree species, predominantly coniferous forests, and mixed forests dominated by broadleaves, including beech, oak, fir, spruce, larch, black pine, red pine, and hornbeam [55,59]. These forests provide diverse habitats for a variety of fauna including mammals like deer, birds, insects, and cricetids [55,59,60].

2.2. Data collection, processing and analysis

Fig. 2 illustrates the research methodology, encompassing imagery acquisition and pre-processing, training of samples, image corrections, supervised classification, accuracy assessment, change detection, as well as forest cover estimation based on vegetation indices.

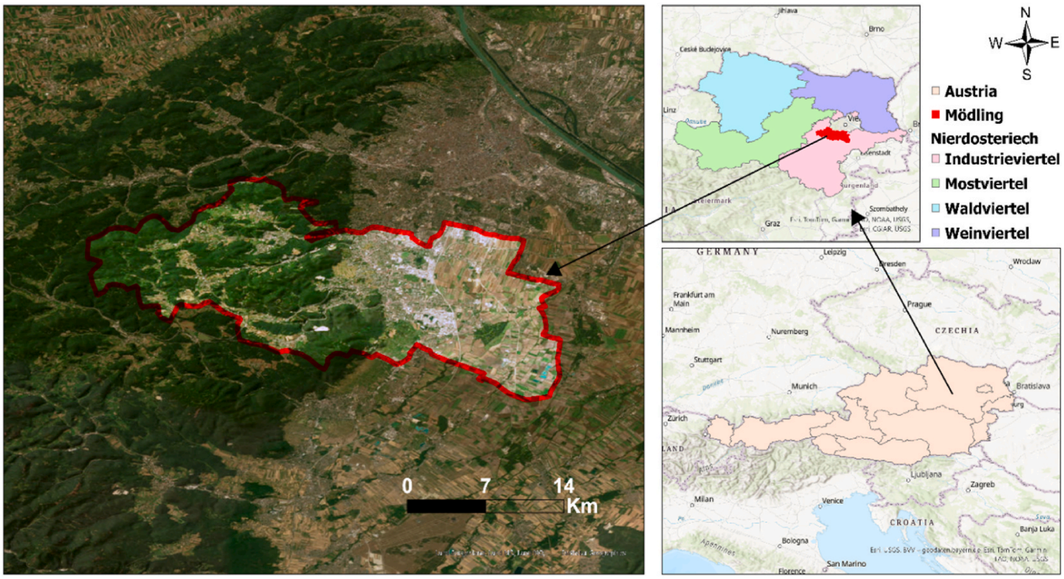

Fig. 1. Map of Austria showing the four regions in Lower Austria (Industrieviertel, Mostviertel, Waldviertel, and Weinviertel), and the study area (Mödling).

2.2.1. Imagery acquisition

Landsat imagery was used for this study. Due to the time steps involved, which cover 1999–2022, two variations of Landsat imagery were utilized. Landsat 7 Enhanced Thematic Map Plus (ETM+) was acquired for 1999 and 2003, while Landsat 8 Optical Land Imaging (OLI) – Thermal Infrared Sensor (TIRS) was obtained for 2013 and 2022 (Table 1). The rationale behind this selection is that the OLI-TIRS sensor for land surface observation started in 2013 – rendering it unavailable for the earlier periods under examination in this study (1999 and 2003). Hence, the ETM + sensor was employed, as it provides imagery dating back to April 1999, rendering it suitable for these two early periods. Beyond considerations of sensor changes and technological advances, the choice to adopt irregular time intervals in data acquisition was based on the availability of high-quality data and the necessity to analyze long-term patterns encompassing specific periods of significance in Austria's LULC dynamics. All images were acquired during the late spring (May) and summer months (June, July, and August). While we acknowledge the potential bias that may result from the data source not covering all the seasons, we ensured that these selected images corresponded to the periods with the highest sunlight and optimal reflection of the infrared wave (band 4 in Landsat 7 and band 5 in Landsat 8) by vegetation. These months align with the peak growth and significant phenological changes in vegetation, coinciding with Austria's agricultural growing period and rainy season, providing a comprehensive representation of the seasonal dynamics for the analysis of various LULC classes. Moreover, the selected images from these periods experienced the least atmospheric interference, ensuring the highest data quality and accessibility for the study. This approach minimizes potential bias, improves land cover classification accuracy, and ensures optimal estimation through vegetation indices.

In addition, images collected during the summer have less cloud cover, which is vital for accurately estimating various land cover characteristics. A reconnaissance survey was further conducted, involving a thorough examination of the study area's environment. Point samples representing different land cover classes were obtained using global positioning systems (GPS). This process allowed us to compare the ground data acquired during the survey with observations from remotely sensed imagery, such that we could obtain information that would provide optimal guidance for effective training of samples for the supervised classification.

2.2.2. Imagery preprocessing

Earth data acquisition by sensors is subject to various limitations and can be affected by atmospheric distortions. Therefore, comparing imagery sourced from different sensors requires image preprocessing and corrections to minimize the effect of cloud cover and other atmospheric disturbances. To achieve this, the direct reflection of land cover features recorded by the sensor – often referred to as the Digital Number (DN) values, in the acquired images was converted to top-of-atmosphere reflectance. This conversion was aimed at reducing the influence of cloud and other atmospheric distortions on the images, ensuring that they could be compared effectively across different sensors. Additionally, a correction for sun angles was applied to the converted images to minimize the effect of varying sun angles during imagery collection on different dates. These corrected images were subsequently used for conducting supervised land cover classifications and for deriving vegetation spectral indices (i.e., NDVI and SAVI) used in this analysis – employing these equations as proposed by Huete [39] and Huang [40].

$$TOA\ Reflectance = \text{Reflectance multi band x DN values} + \text{Reflectance add band} \tag{1}$$

$$Sun\ angle\ correction = \frac{TOA\ Reflectance}{\sin(\text{Sun elevation})} \tag{2}$$

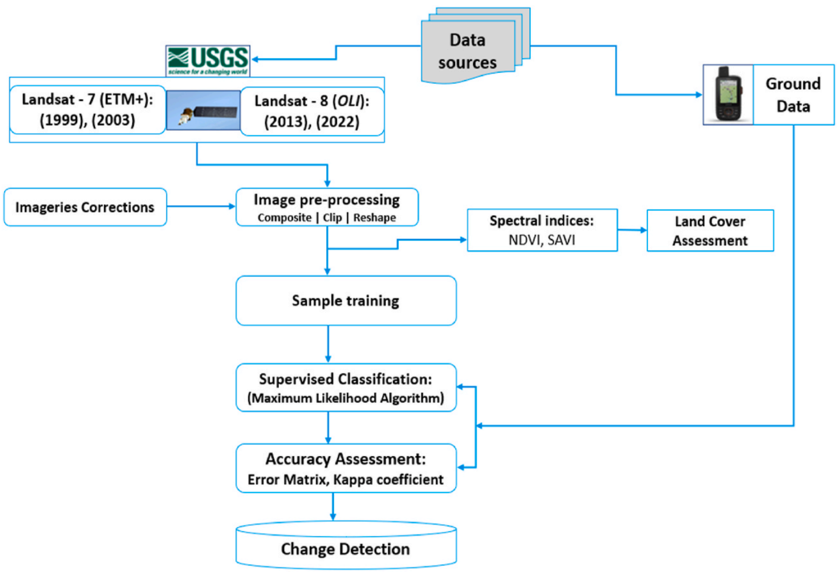

Fig. 2. Flowchart illustrating the sequential stages of the methodology.

Table 1
Imagery sources used in this study: collection dates, path/row, satellite and sensor types, resolutions, and bandwidths.

Year	Collection date (dd/mm/yyyy)	Path/Row	Satellite	Sensor	Resolution (m)	Bandwidth (μm)
1999	07/08/1999	190/027	Landsat-7	ETM+	30	B2 (Green): 0.52–0.60 B3 (Red): 0.63–0.69 B4 (NIR): 0.77–0.90 B7 (SWIR): 2.09–2.35
2003	30/05/2003	190/027	Landsat-7	ETM+	30	B2 (Green): 0.52–0.60 B3 (Red): 0.63–0.69 B4 (NIR): 0.77–0.90 B7 (SWIR): 2.09–2.35
2013	11/06/2013	190/027	Landsat-8	OLI-TIRS	30	B3 (Green): 0.53–0.59 B4 (Red): 0.64–0.67 B5 (NIR): 0.85–0.88 B7 (SWIR): 2.11–2.29
2022	13/07/2022	190/027	Landsat-8	OLI-TIRS	30	B3 (Green): 0.53–0.59 B4 (Red): 0.64–0.67 B5 (NIR): 0.85–0.88 B7 (SWIR): 2.11–2.29

$$NDVI = \frac{NIR - \mathrm{RED}}{\mathrm{NIR} + \mathrm{RED}} \tag{3}$$

$$SAVI = \frac{\mathrm{NIR} - \mathrm{RED}}{\mathrm{NIR} + \mathrm{RED} + \mathrm{L}} \text{ x } (1 + \mathrm{L}) \tag{4}$$

where: NIR = Near Infrared Band; RED: Red Band; the TOA reflectance is the top of the atmosphere reflectance without solar angle correction; reflectance multi-band and add band refer to the band-specific multiplicative and additive rescaling factors, respectively, both obtained from the imagery metadata; the sun angle correction provides the final top-of-atmosphere planetary reflectance used for the analysis. We further analyzed the outputs of the vegetation indices and removed outliers to improve the accuracy of computations and forest cover estimation.

2.2.3. False colour composite

The false colour composite identifies different land cover features based on their reflective intensity in the electromagnetic spectrum's Near Infrared band (NIR). Typically, green surfaces, such as agricultural and forest areas, absorb light in the red and blue bands while reflecting light in the green band of the spectrum, resulting in the green colour visible to the human eye. They also tend to reflect NIR light, which, when combined with visible bands, enables the visualisation of wavelengths that are not visible to the human eye. This distinctive reflectance pattern across the electromagnetic spectrum enables the differentiation of various land cover surfaces. The false colour composite of Mödling for 2022 (Fig. 3) reveals the different land cover characteristics within the study area. Specifically, five land cover classes can be distinguished in the imagery: forested and dense vegetation appears as deep red, agricultural and grassland areas have a lighter red hue compared to forests, water bodies such as lakes and ponds are represented in deep blue and sky blue, bare ground exhibits a slight green tint, and buildings are depicted in cyan. These variations in reflection aided the training of

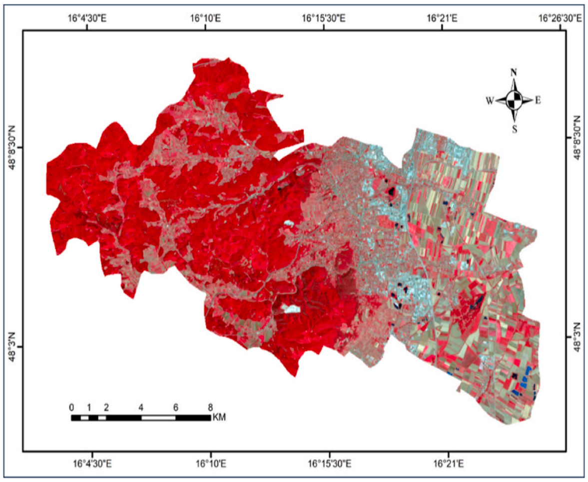

Fig. 3. False colour composite 2022 for Mödling.

samples for the subsequent supervised classification of the images.

2.2.4. Training of samples and image classification

Supervised classification of multitemporal imagery is widely recognized as one of the most effective, well-established, and prevalent techniques for LULC classification, quantification, and change detection. This approach relies on the utilization of training samples and predefined classes [61]. Among the various supervised classification algorithms available, the maximum likelihood classifier stands out as the most extensively employed method in numerous prior studies focused on LULC classification due to its comparatively higher accuracy [62,63]. Therefore, in this study, we adopted the supervised maximum likelihood algorithm to classify the LULC and detect the spatiotemporal changes in Mödling. Maximum likelihood classifies imagery features based on the highest statistical probability of every pixel and its spectral value belonging to certain classes defined in the training samples. Due to this feature, the strength of this algorithm lies in having adequate training samples to represent the different features in the images and obtain a satisfactory level of accuracy in feature representation. Furthermore, the combination of feature representation observed from the ground truthing process, local knowledge of the environment, reflections from different Landsat band combinations, and very high-resolution images from Google Earth provided guidance to accurately train samples for running the image classification. Following Al Mamun [64], we utilized the Maximum Likelihood Image Classification toolbar of ArcMap 10.7 to train the samples, create the signature files, compute the spectral signatures, and conduct the classification for each of the images between 1999 and 2022.

2.2.5. Accuracy assessment

The image classification process is incomplete without assessing the accuracy of the classification. Accuracy assessment involves comparing pixel samples from classified imagery features with the ground feature (often known as the reality), which can be obtained from very high-resolution images, to reveal the extent to which the classified land cover classes represent the actual earth observation. Random points ≥ 160 points were generated for each period using the "Create Accuracy Assessments Points" in the Spatial Analyst toolbox of ArcMap 10.7 to ensure optimal representation of individual land cover classes. The random points representing different land cover classes were exported and displayed on Google Earth to compare the classification results with the ground reality. The reference points from Google Earth were verified using the information from the ground truthing to improve the precision of feature representation. The comparison of the maximum general and mutual means of classification results to actual accuracy outcomes for each land cover class, regarded as the error, contingency, or confusion matrix [65,66], was developed for every classified image. It helps to quantify the correct and incorrect classifications for each class. Common pixel-based accuracy statistical measures, including user's accuracy and producer's accuracy, were computed from the matrix at the class level [46,66–68]. The overall accuracy, which provides a standard measure of the reliability of the classified images [66,68], was further obtained for each image using Eq. (5). Overall accuracy is the ratio of correctly classified pixels (often in diagonal) to the total number of reference pixels [69]. Additionally, the Kappa accuracy coefficient, which evaluates how a classification performs better when compared to a random type, was obtained using Eq. (6) as proposed by Petit [70]. Its values range from 0 to 1, with a higher value indicating greater accuracy.

$$\textit{Overall accuracy} = \frac{\text{Number of correctly classified pixels (Diagonal)}}{\text{Total number of reference pixels}} \text{ x } 100 \tag{5}$$

$$\textit{Kappa coefficient } (\mathbf{T}) = \frac{(\text{TS x TCS}) - \sum(\text{Column total x Row total})}{\text{TS}^2 - \sum(\text{column total x Row total})} \text{ x } 100 \tag{6}$$

Where:

TS = Total Samples.

TCS = Total Correctly Classified Samples.

2.2.6. Change detection

Change detection involves the evaluation of the differences between imagery of the same study areas collected on different dates [70,71]. It compares the spatial characteristics of two points within an exact location along a period while controlling variations resulting from variable differences. The understanding and identification of changes on the land surface across different periods have been identified as a practical and crucial requirement for a better understanding of the multidimensional interaction between natural events and human activities, thus facilitating optimal resource planning, allocation, and management [72]. Several change detection methods have been identified across different studies, each adopting different forms of datasets and techniques. Generally, geographic data such as satellite imagery, maps, and aerial images have been widely used in change detection studies [73]. Furthermore, the development of advanced databases, which house a large volume of archival datasets, has aided the development, evaluation, and optimization of several digital change detection methodologies and algorithms for accurate LULC change detection and assessment [74].

A GIS-based change detection technique was adopted in this study. This approach integrates the remote sensing method and GIS to understand the spatial-temporal changes within our study location [72]. The strength of this method, which necessitated its use, is in the ability to incorporate different data sources, with varied accuracy and formats [70,73] into LULC change detection evaluation for long-period intervals [72]. A post-classification change technique was done by overlaying classified maps of different assessment periods to obtain the changes between them. The differences in areas of each land cover class and changes between land cover classes across the study period were further obtained using the equations below:

$$Land\ Cover\ Change\ (Ha) = A_{fy} - A_{iy} \tag{7}$$

$$\%\ Land\ Cover\ Change = \frac{A_{fy} - A_{iy}}{A_{iy}}\ \mathrm{x}\ 100 \tag{8}$$

$$\%\ LULC\ Area = \frac{A_{lu}}{A_m}\ \mathrm{x}\ 100 \tag{9}$$

where:
A_{fy} = Area of land at the latter year
A_{iy} = Area of land at the initial year
A_{lu} = Land cover area
A_m = Area of Mödling

3. Results and discussions

3.1. Accuracy assessment of classified images

Assessing the accuracy and confirming the validity of the resulting classified maps is considered imperative for change detection analysis following LULC classification. Typically, this assessment involves computing classification errors for each category and overall, for each classified image, as well as analyzing class-level user's accuracy (UA), producer's accuracy (PA), and overall Kappa measures [46,75]. Therefore, in this study, we evaluated the classification accuracy of Mödling using confusion matrices and summarized overall (Kappa) accuracy, as presented in Tables 2 and 3, respectively. The observed class-level accuracies ranged from 85 to 100 % across all the assessed periods, demonstrating the high performance and reliability of our land cover classification and classified maps. According to Anderson et al. [75], a standard accuracy value of 85–90 % is recommended for a credible and valid land cover classification. 85 % of our class-based UA and PA values exceeded this standard, with only six values falling below 90 %, primarily in the 2013 and 2022 OLI-TIRS classified images. The lowest UA (85 %) was observed in the classification of water body in 2013, which however still met the credibility threshold. Overall, the classification results were consistent with Anderson et al. [75] standards, indicating good accuracy.

The classification accuracy in our study is further confirmed by the high overall accuracy of 93.75 %, 94.38 %, 93.13 %, and 91.88

Table 2
Accuracy assessment (confusion matrix) for supervised LULC classification of Mödling for the study period (1999–2022).

Year	Predict	Water body	Built-up area	Bare ground	Agriculture/ grassland	Forested area	Total	User accuracy	Producer accuracy
1999	Water body	18	2	0	0	0	20	90	100
	Built-up area	0	28	1	0	2	31	90.32	90.32
	Bare ground	0	1	31	1	0	33	93.94	91.18
	Agriculture/ grassland	0	0	2	33	0	35	94.29	94.29
	Forested area	0	0	0	1	40	41	97.56	95.24
	Total (Producer)	18	31	34	35	42	160	–	–
2003	Water body	19	1	0	0	0	20	95	100
	Built-up area	0	29	0	0	2	31	93.55	96.67
	Bare ground	0	0	30	3	0	33	90.91	96.77
	Agriculture/ grassland	0	0	1	34	0	35	97.14	87.18
	Forested area	0	0	0	2	39	41	95.12	95.12
	Total (Producer)	19	30	31	39	41	160	–	–
2013	Water body	17	2	0	0	1	20	85	100
	Built-up area	0	29	0	1	1	31	93.55	85.29
	Bare ground	0	2	30	1	0	33	90.91	96.77
	Agriculture/ grassland	0	1	1	33	0	35	94.29	91.67
	Forested area	0	0	0	1	40	41	97.57	95.24
	Total (Producer)	17	34	31	36	42	160	–	–
2022	Water body	18	1	1	0	0	20	90	94.74
	Built-up area	0	28	2	1	0	31	90.32	93.33
	Bare ground	0	0	31	2	0	33	93.94	86.11
	Agriculture/ grassland	1	1	2	31	0	35	88.57	86.11
	Forested area	0	0	0	2	39	41	95.12	100
	Total (Producer)	19	30	36	36	39	160	–	–

Table 3
Accuracy matrices for supervised LULC classification.

Period	Overall accuracy (%)	Kappa accuracy
1999	93.75	0.921
2003	94.38	0.929
2013	93.13	0.913
2022	91.88	0.897

%, and excellent Kappa coefficients of 0.921, 0.929, 0.913, and 0.897 for 1999, 2003, 2013, and 2022, respectively. The accuracy evaluation results we obtained are consistent with and even surpass what many other LULC classification or mapping studies have reported [6,46]. The observed good accuracy in our classification study could be ascribed to the maximum likelihood classification technique, which has been reported to provide the best accuracy among other supervised classifiers, including Mahalanobis distance and minimum distance classifiers [62,76]. This was coupled with extensive training sampling to represent different spectral reflections for each class and validation through meticulous ground-truthing. However, it is important to emphasize the potential influence of landscape complexity on classification accuracy. Mödling's landscape is distinctive in that its land cover classes are quite well-defined and easily distinguishable (as evident in the false colour composite, Fig. 3) with forests dominating the western part, built-up areas prevalent around the east-central region, and agricultural patches occupying most of the eastern land areas. This contributed to minimizing misclassification and facilitating accurate classification of the district's land cover.

3.2. LULC classification of Mödling (1999–2022)

The applications of LULC classification of remotely sensed imagery extend beyond the mapping of individual forest environments and changes to analyzing the patterns of larger and more complex geospatial units, including urban and regional landscapes [6,77], like Mödling. In this study, we evaluated and quantified the LULC features and patterns across the Mödling district in Austria over a two-decadal epoch (1999–2022), specifically considering four years −1999, 2003, 2013, and 2022. The four supervised classification raster outputs of the study area for these periods are depicted in Fig. 4, while Table 4 summarizes the statistics of the area covered by each LULC class for the respective years of assessment. We identified and classified the land cover features in this district into five (5) categories: water bodies, built-up areas, bare ground, agriculture/grassland, and forested areas, aligning with several other global LULC studies [21,46,78,79]. These categories are also adapted from and typically correspond to the top-level classes within the European CLC, which is the standardized land cover classification system used in Europe [48].

In 1999, the forested area in Mödling accounted for 39.11 % of the total land cover, covering around 11,139 ha out of 28,484 ha, making it the largest spatial component. This land cover class, along with agricultural areas, which accounted for 25.63 % (7301 ha), and built-up areas, occupying 21.8 % (6209 ha) of the total land surface, constituted the top three dominant land uses within the district during that period (Table 4). By 2003, a slight reduction in forested area was observed, with its land cover accounting for 37.73 % (10,474 ha) of the total land cover. During that period, agricultural areas already covered 10,013 ha, representing over 35 % of the entire district, while built-up areas covered nearly one-quarter of the district's land surface area, i.e., 23.83 %, amounting to 6787 ha

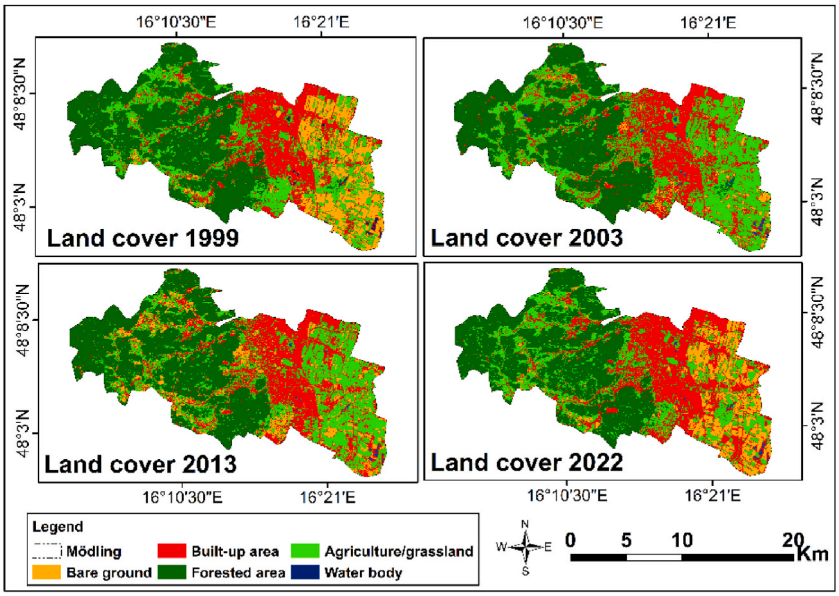

Fig. 4. Supervised land use land cover classification of Mödling for the study periods (1999–2022).

Table 4
LULC area by class and its percentage of the total area (ha) for Mödling (1999–2022).

LULC Class	1999		2003		2013		2022	
	Area (ha)	%	Area (ha)	%	Area (ha)	%	Area (ha)	%
Bare ground	3714.3	13.04	800.91	2.81	2387.7	8.38	3273.21	11.49
Built-up area	6209.91	21.80	6786.99	23.83	7077.78	24.85	7725.42	27.12
Forested area	11139.66	39.11	10747.08	37.73	10593.09	37.19	10396.44	36.50
Agriculture/grassland	7301.52	25.63	10013.85	35.16	8354.07	29.33	7002.36	24.58
Water body	119.43	0.42	135.99	0.48	72.18	0.25	87.39	0.31
Total	28484.82	100	28484.82	100	28484.82	100	28484.82	100

(Table 4). The results of the 2013 LULC classified map showed that forested areas accounted for 37.19 % (equivalent to 10,593 ha) of the total area, maintaining a sizable portion of the district. This was consistently followed by agricultural areas, which occupied 29.33 %, accounting for over 8354 ha, with a less noticeable difference in the spatial extent between these two vegetation-based LULC classes. In that same year (2013), settlement areas had expanded to cover nearly as much land as the agricultural/grassland category, amounting to 24.85 % (~7078 ha) of the total land area in Mödling. According to the most recent classification results in 2022, although forests still consistently occupied the largest area, accounting for a total area of approximately 10,396 ha, representing 36.5 % of the total land area, other classes like built-up areas had evidently started to occupy more land area. Contrasting to previous years, the settlement area had slightly overtaken the agricultural area, covering 3 % of the total land surface, more than the farming and grazing area category. Both classes occupied 7725 ha and 7002 ha, accounting for 27.12 % and 24.58 % of the total district area, respectively (Table 4).

Generally, water bodies occupied the smallest portions of the land cover across the years (1999, 2003, 2013, and 2022), followed by bare soil, when compared to the total land surfaces occupied by other land use classes. Although this observation of the low spatial extent of water bodies could have been partly influenced by the season of data collection, as the images were taken during late spring (May) and summer (June, July, and August) when there was little or no rainfall, Mödling is not typically characterized by extensive water bodies owing to its location in the rugged region of Lower Austria. In 1999, the water bodies covered 0.42 % (119.43 ha) of the land cover area, with 0.48 % (135.99 ha) in 2003, resulting in a 0.06 % expansion in water bodies during that year. Based on the 2013 classification map, that year experienced the lowest coverage of water bodies, occupying only 0.25 % (72.18 ha) of the land surface, while in 2022, the water bodies had reached 0.31 % or 87.39 ha of the total area. Similarly, the bare ground covered a small portion of the land surface around the years, although its pattern was more pronounced than the water body category. The land area covered by bare soil in 1999 was 13.04 % (3714.30 ha) of the total area, but it was only sporadically occupied, 2.81 % (800.91 ha), just about four years later in 2003. As of 2013 and more recently in 2022, bare ground already covered between 8 and 11 % of the total district area, amounting to about 3000 ha (Table 4).

Lower Austrian districts, including Mödling, are renowned for their wide-ranging conventional and organic agricultural production, facilitated by the diverse geography, encompassing fertile plains, hilly areas, and catchment areas [57,80]. Historically, agriculture has been a well-established and prevalent land-use activity in many parts of Mödling, as in other districts within the region [81]. This is evident through the substantial land area, accounting for up to 35 % of the total land area, dedicated to agriculture for the cultivation of grains, oilseeds, fruits, and livestock grazing. However, the spatial coverage of agriculture has decreased in the more recent assessment years when compared to 2003. This trend aligns with the findings of [81] and others who reported and anticipated a reduction in land consumption by agriculture over the years, influenced by agricultural policy changes and settlement expansion. From our findings, in 2022, built-up areas had expanded to cover approximately 28 % of the total land area of the district. This trend is consistent with reports that suggest that built-up areas in Austria have generally experienced a higher rate of growth compared to other EU regions [81]. Nevertheless, we observed that across the assessed periods, forests continued to represent the dominant land cover type in Mödling. Despite the district's location in the industrial quarter hub of Lower Austria and the intensification of settlement, it retains a significant forested area that has remained relatively stable over the years. Most of these forested areas are situated in the western part of the district, while residential areas are primarily located in the transition zone between forests and agricultural lands – pronounced towards the east (see Fig. 4). Mödling's forests transition from lower-elevation montane forests to higher-elevation areas that exhibit characteristics of alpine and subalpine ecosystems. Its forest compositions often include a mix of deciduous tree species like oak (*Quercus* spp.), beech (*Ficus sylvatic*), and maple (*Acer* spp.) and coniferous forest tree species such as Scots pine (*Pinus sylvestris*), Norway spruce (*Picea abies*), Austrian pine (*Pinus nigra*) and among others [55,59].

3.3. LULC change detection for Mödling (1999–2022)

Through geospatial analysis conducted on the LULC classification maps of Mödling, we assessed and quantified the patterns of change in the LULC classes across the evaluation periods (1999–2022). The change detection analysis was carried out for three distinct time frames by developing and analyzing three land area change matrices: 1999–2003, 2003–2013, and 2013–2022, for the Lower Austrian district. Fig. 5 illustrates the class-based change detection outputs, while Fig. 6 and Table 5 present the statistics summarizing the relative changes and corresponding percentages in each cover category in the form of matrices. Additionally, we aimed to comprehend the overall changes within the assessment period by incorporating the 1999–2022 change epoch and evaluating transitions across the cover classes. This was further summarized in Table 6, highlighting the spatiotemporal land cover dynamics in the study area over the past 24 years.

Across the study periods, different LULC types have undergone varying degrees of change in terms of land area (in hectares), with some land cover types experiencing a greater magnitude of change than others (Fig. 5). However, it is noteworthy that the total land area of the district has remained constant, summing up to 28,484.82 ha. While this consistency in spatial land coverage is a common feature in many regions worldwide, there are geographical areas where empirical evidence from remotely sensed change detection indicates a spatiotemporal change in their total land area coverage. For example, in Bahrain, dredging and reclamation activities in the island's shallow water areas have led to an increase in its land area by over 12 % [73]. Furthermore, our analysis revealed that the forested area in Mödling has remained relatively stable for more than two decades, with an overall reduction of −6.67 % (equivalent to 743.22 ha) in forest cover from 1999 to 2022 (Fig. 6 and Table 5). The highest level of forest loss occurred during the shortest epoch, from 1999 to 2003, with a decrease of 392.58 ha, constituting a −3.52 % reduction. In contrast, the decadal period from 2003 to 2013 witnessed the lowest forest loss, with only a −1.43 % reduction in forested areas, amounting to 153.99 ha. This reduction was notably lower than the losses observed in other timeframes, such as the −1.86 % decrease observed between 2013 and 2022 and about −3.5 % in 1999–2003. Interestingly, the most substantial removal and loss of forest cover, experienced between 1999 and 2003, coincided with a considerable expansion in agriculture and grassland. During that period, there was a remarkable increase of over 37 % in the agricultural land area, accounting for 2712.33 ha (Fig. 6 and Table 5). The distinctive accretion in agricultural areas during this period can be partly attributed to the differences in the collection dates of the satellite imagery (Table 1).

The 1999 imagery was acquired in August, coinciding with the harvest season in Lower Austria, which contrasts with the 2003 imagery that was obtained in late May, a period with less harvesting activity. Consequently, this timing difference could have contributed to a relatively high estimate of the agricultural area in 2003. It is understandable that agricultural production and harvesting in Lower Austria, as well as in other areas worldwide, can be estimated using multispectral imagery by selecting images corresponding to periods before and after harvesting. Nevertheless, we established that the earliest period witnessed the most substantial agricultural expansion compared to the subsequent years, as it was the closest to the agricultural industrialization era (1950–1995) across Austria. Since around 2000, changes in agricultural policy and modernization efforts across the country, including our study region, have discouraged agricultural overproduction. Instead, they have facilitated improved agricultural land consumption and sustainable land use practices, partly culminating in a declining trend in cropland and grassland areas [81,82], as evident in our change detection results. By 2022, approximately −4.10 % of the agricultural land area in Mödling, equivalent to 299.16 ha, had been lost relative to the year 1999.

Furthermore, we observed a combination of increasing and decreasing trends in the region's water bodies, with the most substantial change being a loss of approximately 63 ha between 2003 and 2013. This decline can be partly attributed to climate change impacts on the water balance, as many water bodies were recorded to have dried up during this period [83,84]. The situation was exacerbated by the historically severe heatwave in 2003, which occurred two months after our 2003 imagery was captured. Also, Lower Austria experienced several drought episodes within this period, likely contributing to higher evaporation rates and the expansion of bare land areas. However, there appears to have been an improvement in hydrological management practices in the region in the recent decade (2013–2022), as highlighted by Muskoya et al. [57] and Funk et al. [85], which may have contributed to an increase in water bodies. The region has also experienced a series of extreme flood events, potentially influenced by shifts in climate patterns and the dynamics of the Lower Austrian Danube River Basin [86].

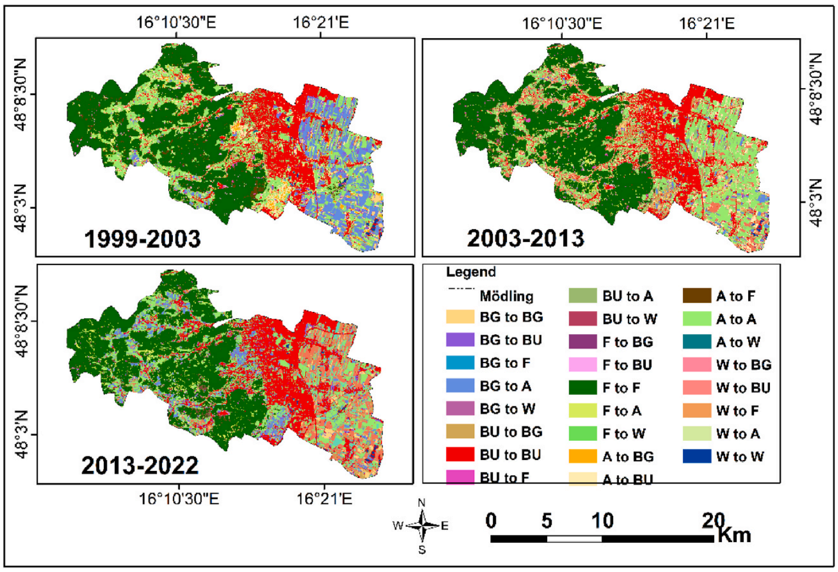

Fig. 5. Class-based land cover changes between study periods (BG = Bare ground, BU = Built-up area, F = Forested area, A = Agriculture/grassland, W = Water body).

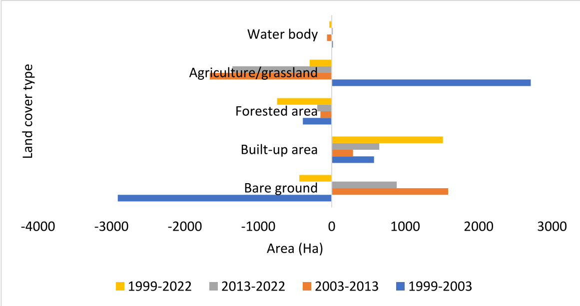

Fig. 6. Land cover changes across study years (1999–2022).

Table 5
Land cover changes and percentages in Mödling across study periods (1999–2022).

LULC	1999–2003		2003–2013		2013–2022		1999–2022	
	Area (ha)	%	Area (ha)	%	Area (ha)	%	Area (ha)	%
Bare ground	−2913.39	−78.44	1586.79	198.12	885.51	37.09	−441.09	−11.88
Built-up area	577.08	9.29	290.79	4.28	647.64	9.15	1515.51	24.40
Forested area	−392.58	−3.52	−153.99	−1.43	−196.65	−1.86	−743.22	−6.67
Agriculture/grassland	2712.33	37.15	−1659.78	−16.57	−1351.71	−16.18	−299.16	−4.10
Water body	16.56	13.87	−63.81	−46.92	15.21	21.07	−32.04	−26.83

Table 6
Cross-tabulation of class-based change detection between 1999 and 2022.

LULC	Period	Water body	Built-up area	Bare ground	Agriculture/grassland	Forested area
Water body	1999–2003	111.6	3.24	0	3.24	1.35
	2003–2013	72.18	51.12	3.69	4.77	4.23
	2013–2022	71.28	0.9	0	0	0
	1999–2022	86.58	27.99	4.14	0.54	0.18
Built-up area	1999–2003	8.55	4572.63	132.39	1406.97	89.37
	2003–2013	0	4888.26	717.66	1103.4	77.67
	2013–2022	16.11	5628.96	522.36	843.21	67.14
	1999–2022	0.54	5139.99	272.12	707.4	89.46
Bare ground	1999–2003	1.44	682.29	347.94	2680.92	1.71
	2003–2013	0	167.76	242.91	389.43	0.81
	2013–2022	0	643.68	537.66	1191.87	14.49
	1999–2022	0.18	720.54	1918.26	1074.06	1.26
Agriculture/grassland	1999–2003	8.19	1401.39	316.35	5128.56	447.03
	2003–2013	0	1832.49	1387.17	6212.88	581.31
	2013–2022	0	1383.21	2209.32	4273.65	487.89
	1999–2022	0	1658.7	1066.41	4136.4	440.01
Forested area	1999–2003	6.21	127.44	4.23	794.16	10207.62
	2003–2013	0	138.15	36.27	643.59	9929.07
	2013–2022	0	68.67	3.87	693.63	9826.92
	1999–2022	0.09	178.2	11.88	1083.96	9865.53

The most prevalent factor influencing the loss of forest and agricultural land areas in the study area is settlement expansion, driven by population growth, industrialization, and urbanization. Our findings revealed that the built-up area was the only LULC type in the district that consistently gained more areas throughout the study period. The expansion in built-up areas had been substantial since the earliest period (1999–2003), with a 9.29 % gain, equivalent to 577.08 ha. Within the subsequent decade (2003–2013) and the most recent period (2013–2022), Mödling's settlements continued to experience a substantive expansion by 290.79 ha and 647.64 ha, accounting for relative increases of 4.28 % and 9.15 %, respectively. Cumulatively, the change in the built-up area amounted to over 1515 ha, representing a 24.40 % increase. This observed change aligns with the trend of settlement sprawl and urban development witnessed in several districts across Austria, given that the country's population growth has increased by approximately 9 % over the past two decades and continues to grow at an annual rate of 0.4 % [87]. According to Getzner and Kadi [87], built-up land areas in Austria have increased by 52 % over the past 20 years, which even doubles the rate we observed in Mödling, thus indicating a progressive conversion of vegetation-based LULC types—agriculture and forest cover—into built-up areas for residential, commercial or infrastructure purposes. Aust et al. [88] reported that about 15 % of the agricultural land in an adjacent Austrian community was converted into residential or other types of infrastructure over a span of 50 years. Such urban development necessitates land clearance, which corresponds to the observed incremental expansion in the bare ground category in Mödling, from 2.81 % (800.9 ha) in 2003 to 8.38 % (2387.7 ha) in 2013, and further to 11.49 % (3273.21 ha) in 2022.

It is crucial to note that increasing forest cover loss and rapid settlement development, without adequate urban planning and land resource management, can potentially pose biological impacts such as biodiversity loss, environmental impacts including climate change and urban heat islands, as well as socio-economic implications such as agrarian livelihood loss and food insecurity [24,46,89]. Extreme weather events, such as prolonged drought, partly attributed to forest loss, have already been linked to various biotic disturbance agents causing considerable damage and mortality across Austrian forest landscapes, including Mödling's, over the past two decades [90]. For instance, different infestations, such as bark beetle infestations in Norway Spruce forests [91] and Phytophthora outbreaks in European beech forest stands [92], as well as the episodic forest fires during heatwaves and drought periods [93] have contributed to forest damage in Lower Austria and Mödling. These factors could partially explain the observed reduction in forest cover in our study.

Furthermore, we investigated the actual transitions occurring with each LULC class. This involved analyzing how the land area was shifting between certain categories, either gained or converted to another category, through a more perceptible cross-tabulation of land use changes (Table 6). Our pixel-based cross-tabulation analysis of the LULC classes confirmed considerable variations in changes across land cover types and assessment periods, with water bodies exhibiting the least changes and the most remarkable transformations observed in agriculture/grassland and built-up categories. Areas covered with water bodies did not experience much change. However, they lost over 27 ha of their initial cover to built-up areas within the entire assessment period, with only negligible area losses (i.e., 0.18–4.14 ha) to other LULC categories. Many lakes have experienced and are predicted to continue drying up, recording significant negative areal trends and threatening future water availability in and around the study region [83,94]. This phenomenon is attributed to reduced groundwater recharge, heatwaves with decreased rainfall, and drought events during extreme summer in Austria, all of which are exacerbated by climate change effects [84,94,95]. On the other hand, forested lands have undergone conversion to other classes, predominantly agriculture/grassland and built-up areas. The highest forest loss, which occurred between 1999 and 2003, was to agriculture, amounting to a total of 794.16 ha, although it was partially offset by an area gain of at least 447 ha. In subsequent periods, the conversion of forest lands for farming declined to approximately 650 ha, partly due to technological advancements in agriculture, such as precision agriculture and policies promoting sustainable forest and land management. During these periods, especially between 2003 and 2013, there was a relatively increasing conversion of forest lands (138.15 ha) into urban and built-up areas, although the rate of conversion appeared to reduce slightly in the most recent epoch (Table 6).

Conversely, agricultural lands continued to transition into built-up as well as bare ground, likely for future settlement development. Approximately 1832 ha and 1386 ha of agriculture/grassland were converted to built-up areas and barren land, respectively, between 2003 and 2013 (Table 6). Despite having gained more land area, cumulatively from all other LULC categories than it lost during the earliest period (1999–2003), agricultural lands continued to give way to the expansion of bare soil and settlements at a substantial degree. The pressure for human settlement in Mödling, as in other Austrian districts, is expected to become increasingly prominent, especially given the high average daily land consumption rate of about 26 ha across the country [87]. A considerable portion of Austrian land is considered sealed and marginal due to its predominantly mountainous and alpine terrains, coupled with the fact that land consumption has increased by more than 50 % over the past two decades [87]. These conditions might incite further degradation of forested lands, as a sizeable expanse of existing agricultural land available for farming is already being heavily consumed and developed for settlements. The ongoing demand for land to support food production could intensify the conversion of forested areas.

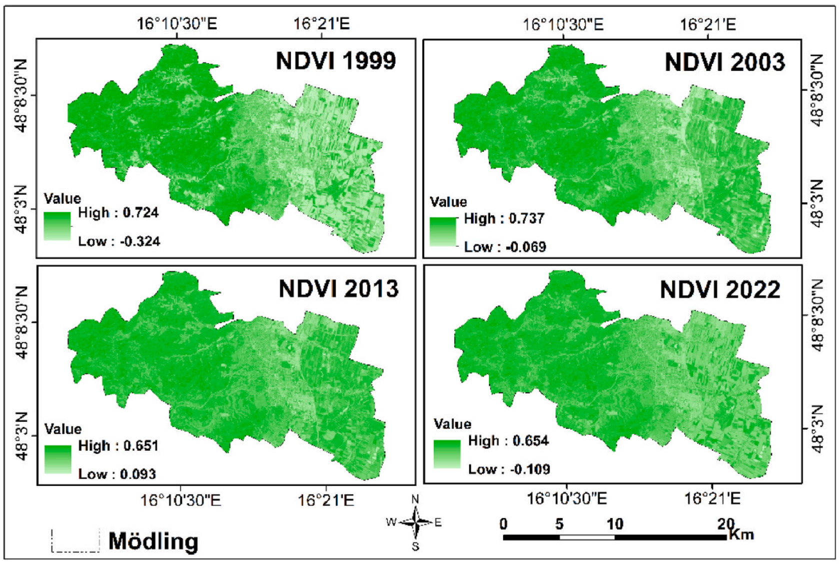

Fig. 7. NDVI of Mödling for the study periods (1999–2022).

Our findings are consistent with several other global LULC studies that have observed land cover transformation for settlement and building use as a primary factor driving LULC dynamics, which is aggravated by population growth, urbanization, human migration and intrusion, and increasing pressure on local communities to meet their habitation needs [6,24,46,73,79,96].

3.4. Vegetation indices

Normalized difference vegetation index has been widely used to assess green production, vitality, and changes in vegetation cover [97] by quantifying the relationship between the differences in spectral reflectance and vegetation growth rate [98]. Regarding the vegetation cover in Mödling, the NDVI results for the four study periods are depicted in Fig. 7. The index values for the district ranged from +0.737 to −0.324, with higher positive values indicating the presence of dense vegetation, while low NDVI values represent sparse vegetation [30,46]. A reduction in dense vegetation, indicating forest cover, was observed across the study period. Specifically, the maximum NDVI value decreased from +0.724 in 1999 to +0.654 in 2022, resulting in a 9.7 % reduction in the maximum NDVI value. However, a slight increase of +0.01 was initially observed between 1999 and 2003, while a minute increase of +0.003 was noted between 2013 and 2022. The most considerable decrease in the maximum value occurred between 2003 and 2013, with a total reduction of 11.7 % from +0.737 to +0.651. Overall, this vegetation index revealed a general decrease in vegetation cover in Mödling across the study period, which aligns with several other NDVI-based LULC mapping studies [6,30,46,99]. The further estimation of forest cover from the NDVI was based on selecting an NDVI threshold to represent dense vegetation in Mödling. Several NDVI values have been used for this purpose, with most values above +0.3 [46,99]. In our case, we selected the value based on the inspection of the value representation of feature classes in each pixel based on extensive information obtained from the ground truthing process. Finally, pixels with values ≥ 0.55 were selected as representative of forest cover.

SAVI, developed by Huete [39], is employed to estimate vegetation cover while minimizing the influence of soil brightness in vegetation indices that use near-infrared and red wavelengths like NDVI. It introduces an adjustment value (L) to minimize soil brightness's influence on vegetation estimation. Several studies have used a range of adjusted values for SAVI, with values typically ranging from 0.25 for dense vegetation to 1 for sparsely distributed vegetation [39]. Following this recommendation, we selected an adjustment level of 0.5, a value widely adopted in several literature sources [100], for this study. The resulting SAVI values for the Mödling district across the evaluation periods are presented in Fig. 8, ranging from +0.993 to −0.435. Comparable to the NDVI, a reduction was observed in SAVI values for the district over the study periods, consistent with Hossain et al. [46] and Islam et al. [99]. Although there was an initial increase in both maximum and minimum values between 1999 and 2003 (from +0.975 to +0.993 and −0.435 to −0.093, respectively), the overall maximum SAVI value decreased from +0.975 in 1999 to +0.882 in 2022. The highest change in the maximum value was recorded between 2003 and 2013, with a −0.114 reduction, followed by a slight increase between 2013 and 2022. The minute relative increases in NDVI and SAVI values within the periods 1999–2003 and 2013–2022 can be attributed to the substantial spatial expansion in agriculture cover and potentially improved greenness of forest vegetation, respectively, despite a reduction in forest cover as earlier identified in the supervised change detection. Furthermore, a similar pixel evaluation method used for NDVI was applied to select the forest cover threshold for SAVI. Consequently, pixels with values ≥ 0.7 were classified as forest cover.

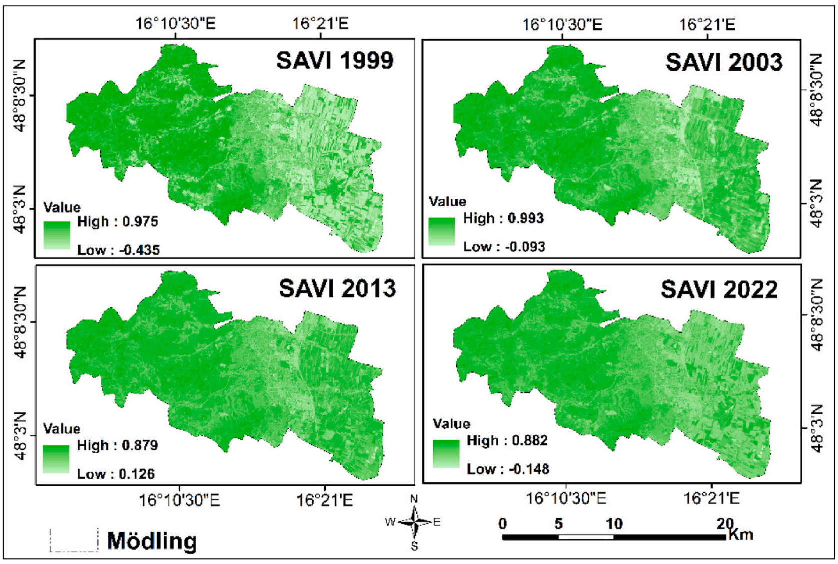

Fig. 8. SAVI of Mödling for the study periods (1999–2022).

Table 7
Forest cover estimates of Mödling from the supervised classification, vegetation indices, and CORINE land cover maps (1999–2022).

Categories	Year							
	1999		2003		2013		2022	
	Area (ha)	(%)	Area (ha)	(%)	Area (ha)	(%)	Area (ha)	(%)
Supervised	11139.66	39.11	10747.08	37.73	10593.09	37.19	10396.44	36.50
NDVI	11159.01	39.18	11430.90	40.13	12240.36	42.97	11398.23	40.02
SAVI	12084.39	42.42	12968.46	45.53	13245.48	46.50	13448.7	47.21
	2000		2006		2012		2018	
CORINE	11050.14	38.79	10989.87	38.58	10991.4	38.59	10982.15	38.55

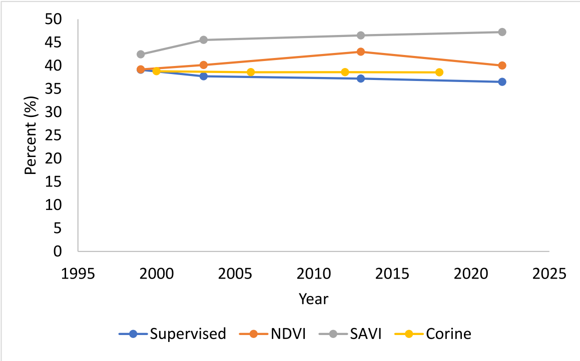

Fig. 9. Percentage of forest area in Mödling across different methods.

3.5. Forest cover estimation based on vegetation indices (NDVI and SAVI) and CORINE land cover

In addition to estimating forest cover through a direct LULC classification process, forest cover quantification and change detection can also be performed using vegetation indices. Direct LULC classification involves accurately determining the appropriate pixel threshold value for the forest class in the respective index. Studies have shown that NDVI and SAVI have the potential to assess forest cover distribution and changes [46,99]. Consequently, we applied these two indices (NDVI and SAVI) to quantify the forest cover in Mödling for each assessment period and compared their estimates with the supervised classification outputs and the standard CLC maps, which cover many European countries, including Austria. Our goal was to evaluate the suitability of vegetation indices in assessing and monitoring forest cover in the district and to validate our estimation using the European land cover maps, while also mutually validating the applicability and accuracy of the CLC maps. The CLC maps are relatively static, with available data for the years 2000, 2006, 2012, and 2018, which posed a limitation in directly comparing our estimates to the cover maps due to the slight mismatch in assessment periods. Nevertheless, this analysis helped visualize the potential comparative trends in forest cover changes over the past two decades using different methods (Table 7 and Fig. 9).

Our results showed that the supervised classification estimated a total forest cover of 11,139 ha in 1999, accounting for 39.1 % of the total land use in the region. This estimate closely matched with the forest cover estimate from NDVI – 11,159 ha or 39.18 % of Mödling's land area. However, the estimated forest cover from SAVI in 1999 exceeded both NDVI and supervised classification, totalling 12,084 ha or 42.2 % of the land area (Table 7). When examining forest cover changes between 1999 and 2003, the supervised classification revealed a reduction to 10,747 ha, representing 37.7 % of the total land cover. In contrast, NDVI and SAVI estimates indicated an increase in forest cover by 2003. Hence, NDVI estimated a total forest cover of 11,431 ha (40.13 %), while SAVI reported 12,968 ha (45.53 %). A similar trend was observed between 2003 and 2013, with supervised classification showing a slightly lower reduction in forest cover, while NDVI and SAVI still overestimated the forest area, indicating an increase. Specifically, NDVI and SAVI evaluated a total forest cover of 12,240 ha (42.97 %) and 13,245 ha (46.50 %), respectively, while the supervised classification only detected a forest cover of 10,593 ha in 2013. A different trend was observed in the forest cover estimation obtained in 2022, with both supervised classification and NDVI showing a decline in forest cover, while SAVI continued to estimate an expansion. A total forest cover of 10,396 ha was calculated from the supervised classification, while NDVI reported a total forest cover of 11,398 ha, and SAVI estimated 13,448 ha of forest cover in the study area (Table 7 and Fig. 9).

Overall, there is a noticeable trend of continuous increase in forest cover estimates obtained from SAVI throughout the study periods, consistently deviating from the supervised classification, which detected a slight decrease in forest cover across the periods. On the other hand, although NDVI also overestimated the forest cover of Mödling, its estimates were still more closely aligned with the supervised classification estimates for most years, except for 2013. These biases in forest cover estimation are consistent with findings from other studies, which have reported varying levels of underestimation or overestimation of forest area using these indices [46,99].

According to Hossain et al. [46], these biases may arise due to the sensitivity of the vegetation indices to factors such as soil reflectance, atmospheric effects, clouds, and vegetation extent. However, if either of these indices were to be considered for a quick forest cover assessment and monitoring in Mödling, preference should be given to NDVI over SAVI due to its relatively smaller deviations, aligning with some previous reports [46,99,101]. In contrast, da Silva et al. [45] found SAVI to be comparatively more adequate, especially for assessing planted forests, agricultural areas, and native fields.

The forest cover estimates from the available CLC maps revealed a slight decrease in forest cover from 2000 to 2018. To be precise, a total forest cover of 11,050 ha was estimated in 2000, 10,989 ha in 2006, 10,991 ha in 2012, and 10,982 ha in 2018 (Table 7 and Fig. 9). The observed similar reducing trend of forest cover estimation from the CLC maps further confirms the performance of our supervised classification results over the vegetation indices. It may be somewhat challenging to perfectly ascertain the accuracy of the European CLC maps in analyzing long-term land cover changes in Mödling and other local European landscapes due to recognized shortfalls attributed to methodological changes in production and periodic static availability of the cover maps [47,51,52]. However, we can infer and validate the forest cover estimation accuracy of the CLC system from the near convergence of the forest cover estimates of our supervised classification in 2013 (10,593 ha) and the CLC map in 2012 (10,991 ha), contrary to other validation studies that have reported greater levels of estimation errors by the European cover maps [51,53,102].

Our findings suggest that temporal changes in CORINE production techniques do not significantly impact accuracy in Mödling, given their temporal consistency with our supervised technique. Meanwhile, Martínez-Fernández [51] asserted that the accuracy and consistency of estimations in CORINE cover maps vary depending on the country and the complexity, fragmentation, and heterogeneity of the assessed landscape. Waser and Schwarz [53] also discovered that the relative accuracy of CORINE maps is contingent on the type of reference maps used for comparison. Their use of MODIS-based land cover products resulted in significant forest area overestimations, in contrast to our higher-resolution Landsat imagery with better accuracies. Nevertheless, we recommend landscape/site-specific supervised classification for a more accurate and contextually appropriate forest cover analysis, as in our study. This approach allows for adequate ground-truthing and assessment of land cover and change events for specific periods of significance in forest cover dynamics, considering the limitation of consistent temporal data availability in the European CLC system. In this process, CLC maps can be utilized to aid in training and analyzing a more extensive set of supervised LULC classes.

4. Conclusions

This study used multispectral imagery to assess LULC changes in the district of Mödling, Lower Austria, over a period of more than two decades (1999–2022). The land cover classes identified within the district include water bodies, built-up areas, bare ground, agriculture/grasslands, and forests. The overall accuracies and Kappa coefficients of the classified images ranged from 91.8 % to 94.3 % and from 0.897 to 0.929, respectively, demonstrating credible classification results in this study. The forested area in the district experienced a reduction in cover over the evaluation period, although this was not very substantial. Forest cover, which initially accounted for over 39 % of the total land area, decreased to approximately 36 % by 2022, resulting in a loss of nearly 750 ha. The highest forest loss occurred in the earliest period of assessment (1999–2003), accounting for a −3.52 % cover reduction. Initially, forest loss led to the accretion of agricultural land during this period. However, in subsequent epochs, both forest and agricultural land areas were converted for settlement expansion, which became the most prevalent factor for LULC changes in the district. Consequently, the continuous expansion of built-up areas in the region, driven by a sporadic increase in population, industrialization, and urbanization in the Lower Austrian industrial quarter (Industrieviertel), has not only resulted in a reduction in forest and other vegetation with potential climate and biodiversity impacts but also reduced agricultural land availability and related livelihood potential for the people in the area.

Furthermore, this study demonstrates the suitability of vegetation indices (NDVI and SAVI) for mapping LULC changes and estimating forest cover, as validated by supervised classification and the CORINE land cover maps. The NDVI and SAVI values for the district were observed to range from +0.74 to −0.32 and + 0.99 to −0.43, respectively. Both indices also exhibited an average decline over the study period, confirming the results of supervised change detection. However, during certain assessment periods, both indices overestimated forest cover in the district. NDVI outperformed SAVI, indicating its superior applicability for rapid vegetation analysis and monitoring in Mödling. Our study revealed consistency between the European CORINE cover maps and our supervised classification outputs, suggesting overall precision and confidence in utilizing both methodologies for LULC analysis. However, we emphasize a preference for a dynamic, context-specific land cover classification over static cover maps derived from a continental database whenever feasible. Lastly, given the observed expansion of settlements in our study, we recommend the implementation of effective measures to regulate and ensure the sustainability of built-up expansion. In addition, advancing policy instruments that promote sustainable forest and agricultural land management practices, such as zoning, land-use planning, and other relevant market-based mechanisms, is crucial for long-term environmental and economic stability. The results of our study are important as they provide evidence-based insights to support decision-making for effective monitoring and policy development related to vegetation conservation, urban development, and overall land management, particularly in peri-urban areas like Mödling.

CRediT authorship contribution statement

Gbenga Lawrence Alawode: Writing – review & editing, Writing – original draft, Visualization, Validation, Methodology, Investigation, Formal analysis, Data curation, Conceptualization. **Tomiwa Victor Oluwajuwon:** Writing – review & editing, Writing – original draft, Validation, Methodology, Investigation, Formal analysis, Conceptualization. **Rasheed Akinleye Hammed:** Writing – review & editing, Writing – original draft, Validation, Formal analysis, Visualization. **Kehinde Ezekiel Olasuyi:** Writing – review &

editing, Writing – original draft, Validation. **Andrey Krasovskiy:** Writing – review & editing, Validation, Supervision. **Oluwadamilola Christianah Ogundipe:** Writing – review & editing, Validation. **Florian Kraxner:** Writing – review & editing, Validation, Supervision.

Ethical statement

This research adhered to established ethical standards for scientific investigation and did not involve human participants or animal subjects at any stage of the study.

Data availability statement

Datasets utilized in the study are freely available on the website of the United States Geological Survey (https://earthexplorer.usgs.gov/).

Funding

This research was conducted as part of the Erasmus Mundus Master's program in European Forestry (MSc EF) funded by the European Commission.

Declaration of competing interest

The authors declare that they have no known competing financial interests or personal relationships that could have appeared to influence the work reported in this paper.

Acknowledgements

This research was also supported at the International Institute for Applied Systems Analysis (IIASA) by the BIOCONSENT project, an international BIODIVERSA + initiative (BiodivRestore 559), financed by the Austrian Science Fund (FWF*)*. The authors are also grateful to Corning Shelby of the IIASA for her valuable insights and constructive feedback, which greatly enhanced the quality of this manuscript. Finally, we deeply appreciate the United States Geological Survey (USGS) for providing free access to the Landsat imagery utilized in this research work.

References

[1] Y. Xie, Z. Sha, M. Yu, Remote sensing imagery in vegetation mapping: a review, J. Plant Ecol. 1 (2008) 9–23, https://doi.org/10.1093/jpe/rtm005.
[2] D.R. Panuju, D.J. Paull, A.L. Griffin, Change detection techniques based on multispectral images for investigating land cover dynamics, Remote Sens. 12 (2020) 1781, https://doi.org/10.3390/rs12111781.
[3] A. Letourneau, P.H. Verburg, E. Stehfest, A land-use systems approach to represent land-use dynamics at continental and global scales, Environ. Model. Software 33 (2012) 61–79, https://doi.org/10.1016/j.envsoft.2012.01.007.
[4] Hadi, A. Krasovskii, V. Maus, P. Yowargana, S. Pietsch, M. Rautiainen, Monitoring Deforestation in Rainforests Using Satellite Data: A Pilot Study from Kalimantan, Indonesia, Forests 9 (2018) 389, https://doi.org/10.3390/f9070389.
[5] A.H. Chughtai, H. Abbasi, I.R. Karas, A review on change detection method and accuracy assessment for land use land cover, Remote Sens. Appl.: Society and Environment 22 (2021) 100482, https://doi.org/10.1016/j.rsase.2021.100482.
[6] S. Hussain, L. Lu, M. Mubeen, W. Nasim, S. Karuppannan, S. Fahad, A. Tariq, B.G. Mousa, F. Mumtaz, M. Aslam, Spatiotemporal variation in land use land cover in the response to local climate change using multispectral remote sensing data, Land 11 (2022) 595, https://doi.org/10.3390/land11050595.
[7] M.A. Mohamed, Monitoring of temporal and spatial changes of land use and land cover in metropolitan regions through remote sensing and GIS, NR 08 (2017) 353–369, https://doi.org/10.4236/nr.2017.85022.
[8] Maulana Azad National Institute of Technology, Bhopal, India, S. Mishra, P. Shrivastava, Maulana azad national institute of technology bhopal, in: P. Dhurvey, Maulana Azad National Institute of Technology, Bhopal, India, Change Detection Techniques in Remote Sensing: a Review, IJWMCIS, 2017, pp. 1–8, https://doi.org/10.21742/ijwmcis.2017.4.1.01, 4.
[9] Soil and water conservation Engg, Department, dr. PDKV, Akola, M.H. (444 001), India, S. Chaware, N. Patil, national bureau of soil survey and land use planning, amravati road, Nagpur, M.H. (440 033), India, G. Satpute, soil and water conservation Engg. Department, Dr. PDKV, Akola, M.H. (444 001), India, M.R. Meshram, central institute for cotton research, Wardha road, Nagpur, M.H. (440 010), India, A spatio-temporal study of land use land cover change detection using GIS and remote sensing techniques, IJBSM 12 (2021), https://doi.org/10.23910/1.2021.2138b, 026–031.
[10] A. Sharma, X. Liu, X. Yang, Land cover classification from multi-temporal, multi-spectral remotely sensed imagery using patch-based recurrent neural networks, Neural Netw. 105 (2018) 346–355, https://doi.org/10.1016/j.neunet.2018.05.019.
[11] N. Ahmad, Spatio-temporal change detection analysis of land use land cover of bathinda district, Punjab, India, Biosci. Biotechnol. Res. Asia 20 (2023) 571–590, https://doi.org/10.13005/bbra/3111.
[12] Department of Geography, Bangalore University, India, A. Younes, A. Ahmad, Department of civil engineering, Indian institute of technology Guwahati, India, A.D. hanjag, department of geography, Bangalore university, India, A.M. Nair, department of civil engineering, Indian institute of technology Guwahati, India, understanding dynamics of land use & land cover change using GIS & change detection techniques in tartous, Syria, EJG 14 (2023) 20–41, https://doi.org/10.48088/ejg.a.you.14.3.020.041.
[13] W. Wang, C. Zhang, J. Allen, W. Li, M. Boyer, K. Segerson, J. Silander, Analysis and prediction of land use changes related to invasive species and major driving forces in the state of Connecticut, Land 5 (2016) 25, https://doi.org/10.3390/land5030025.
[14] P.C. Pandey, N. Koutsias, G.P. Petropoulos, P.K. Srivastava, E. Ben Dor, Land use/land cover in view of earth observation: data sources, input dimensions, and classifiers—a review of the state of the art, Geocarto Int. 36 (2021) 957–988, https://doi.org/10.1080/10106049.2019.1629647.
[15] C. Schweitzer, J.A. Priess, S. Das, A generic framework for land-use modelling, Environ. Model. Software 26 (2011) 1052–1055, https://doi.org/10.1016/j.envsoft.2011.02.016.

[16] P. Potapov, M.C. Hansen, A. Pickens, A. Hernandez-Serna, A. Tyukavina, S. Turubanova, V. Zalles, X. Li, A. Khan, F. Stolle, N. Harris, X.-P. Song, A. Baggett, I. Kommareddy, A. Kommareddy, The global 2000-2020 land cover and land use change dataset derived from the landsat archive: first results, front, Remote Sens. 3 (2022) 856903, https://doi.org/10.3389/frsen.2022.856903.

[17] M.A. Zoran, R. Savastru, D. Savastru, M. Tautan, S. Miclos, Multispectral and multitemporal satellite remote sensing imagery for Bucharest land cover dynamics assessment, in: V.I. Vlad (Ed.), Sibiu, Romania, 2009, p. 74690Q, https://doi.org/10.1117/12.861526.

[18] M. Amani, A. Ghorbanian, S.A. Ahmadi, M. Kakooei, A. Moghimi, S.M. Mirmazloumi, S.H.A. Moghaddam, S. Mahdavi, M. Ghahremanloo, S. Parsian, Q. Wu, B. Brisco, Google Earth engine cloud computing platform for remote sensing big data applications: a comprehensive review, IEEE J. Sel. Top. Appl. Earth Obs. Rem. Sens. 13 (2020) 5326–5350, https://doi.org/10.1109/JSTARS.2020.3021052.

[19] A. Akodéwou, J. Oszwald, S. Saïdi, L. Gazull, S. Akpavi, K. Akpagana, V. Gond, Land use and land cover dynamics analysis of the togodo protected area and its surroundings in southeastern Togo, West Africa, Sustainability 12 (2020) 5439, https://doi.org/10.3390/su12135439.

[20] B. Sajan, V.N. Mishra, S. Kanga, G. Meraj, S.K. Singh, P. Kumar, Cellular automata-based artificial neural network model for assessing past, present, and future land use/land cover dynamics, Agronomy 12 (2022) 2772, https://doi.org/10.3390/agronomy12112772.

[21] S. Hussain, M. Mubeen, A. Ahmad, W. Akram, H.M. Hammad, M. Ali, N. Masood, A. Amin, H.U. Farid, S.R. Sultana, S. Fahad, D. Wang, W. Nasim, Using GIS tools to detect the land use/land cover changes during forty years in Lodhran district of Pakistan, Environ. Sci. Pollut. Res. 27 (2020) 39676–39692, https://doi.org/10.1007/s11356-019-06072-3.

[22] I. Ouedraogo, P. Savadogo, M. Tigabu, R. Cole, P.C. Oden, J.-M. Ouadba, Trajectory analysis of forest cover change in the tropical dry forest of Burkina Faso, West Africa, Landsc. Res. 36 (2011) 303–320, https://doi.org/10.1080/01426397.2011.564861.

[23] X. Deng, Z. Li, A review on historical trajectories and spatially explicit scenarios of land-use and land-cover changes in China, J. Land Use Sci. 11 (2016) 709–724, https://doi.org/10.1080/1747423X.2016.1241312.

[24] J.A. Bukoye, T.V. Oluwajuwon, A.A. Alo, C. Offiah, R. Israel, M.E. Ogunmodede, Land use land cover dynamics of Oba hills forest reserve, Nigeria, employing multispectral imagery and GIS, ARS 12 (2023) 123–144, https://doi.org/10.4236/ars.2023.124007.

[25] K. Kern, W. Sulzer, G.K. Lieb, in: U. Michel, D.L. Civco (Eds.), Detection of land-cover and land-use Change in the Hohe Tauern National Park (Austria) Using an Object-based Classification Approach: First Results, 2009 747825, https://doi.org/10.1117/12.829977. Berlin, Germany.

[26] A. Kollert, M. Bremer, M. Löw, M. Rutzinger, Exploring the potential of land surface phenology and seasonal cloud free composites of one year of Sentinel-2 imagery for tree species mapping in a mountainous region, Int. J. Appl. Earth Obs. Geoinf. 94 (2021) 102208, https://doi.org/10.1016/j.jag.2020.102208.

[27] A.R. Huete, K. Didan, A. Huete, K. Didan, W. Van Leeuwen, A. Jacobson, R. Solanos, T. Laing, Modis vegetation index (MOD 13) algorithm theoretical basis document. http://vip.arizona.edu, 1999.

[28] J. Xue, B. Su, Significant remote sensing vegetation indices: a review of developments and applications, J. Sens. 2017 (2017) 1–17, https://doi.org/10.1155/2017/1353691.

[29] K. Solymosi, G. Kövér, R. Romvári, The progression of vegetation indices: a short overview, AAK 23 (2019), https://doi.org/10.31914/aak.2264.

[30] A.R. Huete, Vegetation indices, remote sensing and forest monitoring, Geography Compass 6 (2012) 513–532, https://doi.org/10.1111/j.1749-8198.2012.00507.x.

[31] M. Schultz, J.G.P.W. Clevers, S. Carter, J. Verbesselt, V. Avitabile, H.V. Quang, M. Herold, Performance of vegetation indices from landsat time series in deforestation monitoring, Int. J. Appl. Earth Obs. Geoinf. 52 (2016) 318–327, https://doi.org/10.1016/j.jag.2016.06.020.

[32] B. Almutairi, A. El, M.A. Belaid, N. Musa, Comparative study of SAVI and NDVI vegetation indices in sulaibiya area (Kuwait) using worldview satellite imagery, Int. J. Geosci. Geomat (2013) 50–53. https://www.researchgate.net/publication/299469974.

[33] R. Lugassi, N. Goldshleger, A. Chudnovsky, Studying vegetation salinity: from the field view to a satellite-based perspective, Remote Sens. 9 (2017) 122, https://doi.org/10.3390/rs9020122.

[34] P.P. Rhyma, K. Norizah, O. Hamdan, I. Faridah-Hanum, A.W. Zulfa, Integration of normalised different vegetation index and soil-adjusted vegetation index for mangrove vegetation delineation, Remote Sens. Appl.: Society and Environment 17 (2020) 100280, https://doi.org/10.1016/j.rsase.2019.100280.

[35] N. Shibani, A. Pandey, V. Krishan Satyam, J. Singh Bhari, B. Ahmed Karimi, S. Kumar Gupta, Study on the variation of NDVI, SAVI and EVI indices in Punjab state, India, IOP Conf. Ser. Earth Environ. Sci. 1110 (2023) 012070, https://doi.org/10.1088/1755-1315/1110/1/012070.

[36] I. Markevych, J. Schoierer, T. Hartig, A. Chudnovsky, P. Hystad, A.M. Dzhambov, S. De Vries, M. Triguero-Mas, M. Brauer, M.J. Nieuwenhuijsen, G. Lupp, E. A. Richardson, T. Astell-Burt, D. Dimitrova, X. Feng, M. Sadeh, M. Standl, J. Heinrich, E. Fuertes, Exploring pathways linking greenspace to health: theoretical and methodological guidance, Environ. Res. 158 (2017) 301–317, https://doi.org/10.1016/j.envres.2017.06.028.

[37] P. Fabijańczyk, J. Zawadzki, Spatial correlations of NDVI and MSAVI2 indices of green and forested areas of urban agglomeration, case study Warsaw, Poland, Remote Sens. Appl.: Society and Environment 26 (2022) 100721, https://doi.org/10.1016/j.rsase.2022.100721.

[38] C.J. Tucker, Red and photographic infrared linear combinations for monitoring vegetation, Rem. Sens. Environ. 8 (1979) 127–150, https://doi.org/10.1016/0034-4257(79)90013-0.

[39] A.R. Huete, A soil-adjusted vegetation index (SAVI), Rem. Sens. Environ. 25 (1988) 295–309, https://doi.org/10.1016/0034-4257(88)90106-X.

[40] S. Huang, L. Tang, J.P. Hupy, Y. Wang, G. Shao, A commentary review on the use of normalized difference vegetation index (NDVI) in the era of popular remote sensing, J. For. Res. 32 (2021) 1–6, https://doi.org/10.1007/s11676-020-01155-1.

[41] C. Eisfelder, S. Asam, A. Hirner, P. Reiners, S. Holzwarth, M. Bachmann, U. Gessner, A. Dietz, J. Huth, F. Bachofer, C. Kuenzer, Seasonal vegetation trends for Europe over 30 years from a novel normalised difference vegetation index (NDVI) time-Series—The TIMELINE NDVI product, Remote Sens. 15 (2023) 3616, https://doi.org/10.3390/rs15143616.

[42] C. Small, Estimation of urban vegetation abundance by spectral mixture analysis, Int. J. Rem. Sens. 22 (2001) 1305–1334, https://doi.org/10.1080/01431160151144369.

[43] J. Qi, A. Chehbouni, A.R. Huete, Y.H. Kerr, S. Sorooshian, A modified soil adjusted vegetation index, Rem. Sens. Environ. 48 (1994) 119–126, https://doi.org/10.1016/0034-4257(94)90134-1.

[44] H. Ren, G. Zhou, F. Zhang, Using negative soil adjustment factor in soil-adjusted vegetation index (SAVI) for aboveground living biomass estimation in arid grasslands, Rem. Sens. Environ. 209 (2018) 439–445, https://doi.org/10.1016/j.rse.2018.02.068.

[45] V.S. Da Silva, G. Salami, M.I.O. Da Silva, E.A. Silva, J.J. Monteiro Junior, E. Alba, Methodological evaluation of vegetation indexes in land use and land cover (LULC) classification, Geology, Ecology, and Landscapes 4 (2020) 159–169, https://doi.org/10.1080/24749508.2019.1608409.

[46] MdS. Hossain, MdA.H. Khan, T.V. Oluwajuwon, J. Biswas, S.M. Rubaiot Abdullah, MdS.S.I. Tanvir, S. Munira, MdN.A. Chowdhury, Spatiotemporal change detection of land use land cover (LULC) in Fashiakhali wildlife sanctuary (FKWS) impact area, Bangladesh, employing multispectral images and GIS, Model. Earth Syst. Environ. 9 (2023) 3151–3173, https://doi.org/10.1007/s40808-022-01653-7.

[47] G. Büttner, CORINE land cover and land cover change products, in: I. Manakos, M. Braun (Eds.), Land Use and Land Cover Mapping in Europe, Springer Netherlands, Dordrecht, 2014, pp. 55–74, https://doi.org/10.1007/978-94-007-7969-3_5.

[48] J. Feranec, T. Soukup, G. Feranec, G. Jaffrain (Eds.), European Landscape Dynamics: CORINE Land Cover Data, CRC Press, 2016, https://doi.org/10.1201/9781315372860, 6000 Broken Sound Parkway NW, Suite 300 Boca Raton, FL 33487-2742.

[49] I. Cieślak, K. Szuniewicz, K. Pawlewicz, S. Czyża, Land use changes monitoring with CORINE land cover data, IOP Conf. Ser. Mater. Sci. Eng. 245 (2017) 052049, https://doi.org/10.1088/1757-899X/245/5/052049.

[50] L. Aune-Lundberg, G.-H. Strand, The content and accuracy of the CORINE land cover dataset for Norway, Int. J. Appl. Earth Obs. Geoinf. 96 (2021) 102266, https://doi.org/10.1016/j.jag.2020.102266.

[51] J. Martínez-Fernández, P. Ruiz-Benito, A. Bonet, C. Gómez, Methodological variations in the production of CORINE land cover and consequences for long-term land cover change studies. The case of Spain, Int. J. Rem. Sens. (2019) 1–19, https://doi.org/10.1080/01431161.2019.1624864.

[52] D. García-Álvarez, M.T. Camacho Olmedo, Changes in the methodology used in the production of the Spanish CORINE: uncertainty analysis of the new maps, Int. J. Appl. Earth Obs. Geoinf. 63 (2017) 55–67, https://doi.org/10.1016/j.jag.2017.07.001.

[53] L.T. Waser, M. Schwarz, Comparison of large-area land cover products with national forest inventories and CORINE land cover in the European Alps, Int. J. Appl. Earth Obs. Geoinf. 8 (2006) 196–207, https://doi.org/10.1016/j.jag.2005.10.001.
[54] Amt der NÖ Landesregierung, Wohnbevölkerung 2023 nach Alter und Gemeinden. https://www.NOE.Gv.at/NOE/Index.Html, 2023.
[55] E. Johann, Coppice forests in Austria: the re-introduction of traditional management systems in coppice forests in response to the decline of species and landscape and under the aspect of climate change, For. Ecol. Manag. 490 (2021) 119129, https://doi.org/10.1016/j.foreco.2021.119129.
[56] ZAMG Austrian Central Institute for Meteorology and Geodynamics, Climate of Austria, 2023.
[57] F.K. Musyoka, P. Strauss, G. Zhao, S. Strohmeier, B.M. Mutua, A. Klik, Evaluating the impacts of sustainable land management practices on water quality in an agricultural catchment in Lower Austria using SWAT, Environ. Monit. Assess. 195 (2023) 512, https://doi.org/10.1007/s10661-023-11079-y.
[58] A. Grass, K. Tremetsberger, R. Hössinger, K.-G. Bernhardt, Change of Species and Habitat Diversity in the Pannonian Region of Eastern Lower Austria over 170 Years: Using Herbarium Records as a Witness, NR 05 (2014) 583–596, https://doi.org/10.4236/nr.2014.511051.
[59] J. Huber, L. Ranacher, T. Stern, P. Schwarzbauer, Forest management or greed of gain?—An information experiment on peri-urban forest visitors' attitudes regarding harvesting operations, Urban For. Urban Green. 27 (2017) 214–220, https://doi.org/10.1016/j.ufug.2017.08.005.
[60] G. Daxner-Höck, Cricetinae aus dem alt-Pliozän vom Eichkogel bei Mödling (Niederösterreich) und von Vösendorf bei Wien, Paläontol. Z. 46 (1972) 133–150, https://doi.org/10.1007/BF02990149.
[61] K. Perumal, R. Bhaskaran, Supervised classification performance of multispectral images. http://arxiv.org/abs/1002.4046, 2010. (Accessed 20 April 2024).
[62] P.S. Sisodia, V. Tiwari, A. Kumar, Analysis of supervised maximum likelihood classification for remote sensing image, in: International Conference on Recent Advances and Innovations in Engineering (ICRAIE-2014), IEEE, Jaipur, India, 2014, pp. 1–4, https://doi.org/10.1109/ICRAIE.2014.6909319.
[63] H. Hossen, A. Negm, Change detection in the water bodies of Burullus Lake, northern Nile Delta, Egypt, using RS/GIS, Procedia Eng. 154 (2016) 951–958, https://doi.org/10.1016/j.proeng.2016.07.529.
[64] A. Al Mamun, Identification and monitoring the change of land use pattern using remote sensing and GIS, A Case Study of Dhaka City, IOSR-JMCE 6 (2013) 20–28, https://doi.org/10.9790/1684-0622028.
[65] D. Lu, G. Li, E. Moran, S. Hetrick, Spatiotemporal analysis of land-use and land-cover change in the Brazilian amazon, Int. J. Rem. Sens. 34 (2013) 5953–5978, https://doi.org/10.1080/01431161.2013.802825.
[66] G.M. Foody, Status of land cover classification accuracy assessment, Rem. Sens. Environ. 80 (2002) 185–201, https://doi.org/10.1016/S0034-4257(01)00295-4.
[67] R.G. Congalton, A review of assessing the accuracy of classifications of remotely sensed data, Rem. Sens. Environ. 37 (1991) 35–46, https://doi.org/10.1016/0034-4257(91)90048-B.
[68] R.G. Congalton, K. Green, Assessing the Accuracy of Remotely Sensed Data: Principles and Practices, third ed., third ed., CRC Press, 2019 https://doi.org/10.1201/9780429052729.
[69] J. Rogan, J. Franklin, D.A. Roberts, A comparison of methods for monitoring multitemporal vegetation change using thematic mapper imagery, Rem. Sens. Environ. 80 (2002) 143–156, https://doi.org/10.1016/S0034-4257(01)00296-6.
[70] C.C. Petit, E.F. Lambin, Integration of multi-source remote sensing data for land cover change detection, Int. J. Geogr. Inf. Sci. 15 (2001) 785–803, https://doi.org/10.1080/13658810110074483.
[71] I.R. Hegazy, M.R. Kaloop, Monitoring urban growth and land use change detection with GIS and remote sensing techniques in Daqahlia governorate Egypt, Int. J. Sustain. Built Environ. 4 (2015) 117–124, https://doi.org/10.1016/j.ijsbe.2015.02.005.
[72] D. Lu, P. Mausel, E. Brondízio, E. Moran, Change detection techniques, Int. J. Rem. Sens. 25 (2004) 2365–2401, https://doi.org/10.1080/0143116031000139863.
[73] S.S. Aljenaid, G.R. Kadhem, M.F. AlKhuzaei, J.B. Alam, Detecting and assessing the spatio-temporal land use land cover changes of Bahrain island during 1986–2020 using remote sensing and GIS, Earth Syst Environ 6 (2022) 787–802, https://doi.org/10.1007/s41748-022-00315-z.
[74] KhM. Dewidar, Detection of land use/land cover changes for the northern part of the Nile delta (Burullus region), Egypt, Int. J. Rem. Sens. 25 (2004) 4079–4089, https://doi.org/10.1080/01431160410001688312.
[75] R. Anderson, E.E. Hardy, J.T. Roach, R.E. Witmer, A Land Use and Land Cover Classification System for Use with Remote Sensor Data, 1976.
[76] N.A. Mahmon, N. Ya'acob, A.L. Yusof, Differences of image classification techniques for land use and land cover classification, in: 2015 IEEE 11th International Colloquium on Signal Processing & its Applications (CSPA), IEEE, Kuala Lumpur, Malaysia, 2015, pp. 90–94, https://doi.org/10.1109/CSPA.2015.7225624.
[77] Y.E. Shimabukuro, E. Arai, G.M. Da Silva, T.B. Hoffmann, V. Duarte, P.R. Martini, A.C. Dutra, G. Mataveli, H.L.G. Cassol, M. Adami, Mapping land use and land cover classes in São Paulo state, southeast of Brazil, using Landsat-8 OLI multispectral data and the derived spectral indices and fraction images, Forests 14 (2023) 1669, https://doi.org/10.3390/f14081669.
[78] T.V. Oluwajuwon, A.A. Alo, F.N. Ogana, O.A. Adekugbe, Forest cover dynamics of a lowland rainforest in Southwestern Nigeria using GIS and remote sensing techniques, JGIS 13 (2021) 83–97, https://doi.org/10.4236/jgis.2021.132006.
[79] M.M. Billah, MdM. Rahman, J. Abedin, H. Akter, Land cover change and its impact on human–elephant conflict: a case from Fashiakhali forest reserve in Bangladesh, SN Appl. Sci. 3 (2021) 649, https://doi.org/10.1007/s42452-021-04625-1.
[80] M. Brückler, T. Resl, A. Reindl, Comparison of organic and conventional crop yields in Austria, Die Bodenkultur: Journal of Land Management, Food and Environment 68 (2018) 223–236, https://doi.org/10.1515/boku-2017-0018.
[81] F. Krausmann, H. Haberl, N.B. Schulz, K.-H. Erb, E. Darge, V. Gaube, Land-use change and socio-economic metabolism in Austria—part I: driving forces of land-use change: 1950–1995, Land Use Policy 20 (2003) 1–20, https://doi.org/10.1016/S0264-8377(02)00048-0.
[82] J. Blasch, F. Vuolo, L. Essl, B. Van Der Kroon, Drivers and barriers influencing the willingness to adopt technologies for variable rate application of fertiliser in Lower Austria, Agronomy 11 (2021) 1965, https://doi.org/10.3390/agronomy11101965.
[83] A. Emmer, S. Merkl, M. Mergili, Spatiotemporal patterns of high-mountain lakes and related hazards in western Austria, Geomorphology 246 (2015) 602–616, https://doi.org/10.1016/j.geomorph.2015.06.032.
[84] G. Soja, J. Züger, M. Knoflacher, P. Kinner, A.-M. Soja, Climate impacts on water balance of a shallow steppe lake in eastern Austria (Lake Neusiedl), J. Hydrol. 480 (2013) 115–124, https://doi.org/10.1016/j.jhydrol.2012.12.013.
[85] A. Funk, J. Martínez-López, F. Borgwardt, D. Trauner, K.J. Bagstad, S. Balbi, A. Magrach, F. Villa, T. Hein, Identification of conservation and restoration priority areas in the Danube river based on the multi-functionality of river-floodplain systems, Sci. Total Environ. 654 (2019) 763–777, https://doi.org/10.1016/j.scitotenv.2018.10.322.
[86] M. Weiler, G.G. Duscher, M. Wetscher, J. Walochnik, Tick abundance: a one year study on the impact of flood events along the banks of the river Danube, Austria, Exp Appl Acarol 71 (2017) 151–157, https://doi.org/10.1007/s10493-017-0114-1.
[87] M. Getzner, J. Kadi, Determinants of land consumption in Austria and the effects of spatial planning regulations, Eur. Plan. Stud. 28 (2020) 1095–1117, https://doi.org/10.1080/09654313.2019.1604634.
[88] G. Aust, F. Heinrich, D. Horvath, A. Musil, C. Foldal, R. Jandl, Conversion of agricultural soils in Austria—a case study for a community in Upper Austria, Die Bodenkultur: Journal of Land Management, Food and Environment 71 (2020) 69–76, https://doi.org/10.2478/boku-2020-0007.
[89] K.C. Seto, B. Güneralp, L.R. Hutyra, Global forecasts of urban expansion to 2030 and direct impacts on biodiversity and carbon pools, Proc. Natl. Acad. Sci. USA 109 (2012) 16083–16088, https://doi.org/10.1073/pnas.1211658109.
[90] C. Senf, R. Seidl, Natural disturbances are spatially diverse but temporally synchronized across temperate forest landscapes in Europe, Glob. Change Biol. 24 (2018) 1201–1211, https://doi.org/10.1111/gcb.13897.
[91] S. Netherer, B. Panassiti, J. Pennerstorfer, B. Matthews, Acute drought is an important driver of bark beetle infestation in Austrian Norway spruce stands, Front. For. Glob. Change 2 (2019) 39, https://doi.org/10.3389/ffgc.2019.00039.
[92] T. Corcobado, T.L. Cech, M. Brandstetter, A. Daxer, C. Hüttler, T. Kudláček, M. Horta Jung, T. Jung, Decline of European beech in Austria: involvement of Phytophthora spp. and contributing biotic and abiotic factors, Forests 11 (2020) 895, https://doi.org/10.3390/f11080895.

[93] M. Müller, H. Vacik, E. Valese, Anomalies of the Austrian forest fire regime in comparison with other alpine countries: a research note, Forests 6 (2015) 903–913, https://doi.org/10.3390/f6040903.

[94] K. Haslinger, W. Schöner, J. Abermann, G. Laaha, K. Andre, M. Olefs, R. Koch, Apparent contradiction in the projected climatic water balance for Austria: wetter conditions on average versus higher probability of meteorological droughts, Nat. Hazards Earth Syst. Sci. 23 (2023) 2749–2768, https://doi.org/10.5194/nhess-23-2749-2023.

[95] M.T. Dokulil, Predicting summer surface water temperatures for large Austrian lakes in 2050 under climate change scenarios, Hydrobiologia (The Hague) 731 (2014) 19–29, https://doi.org/10.1007/s10750-013-1550-5.

[96] M. Fasona, P.A. Adeonipekun, O. Agboola, A. Akintuyi, A. Bello, O. Ogundipe, A. Soneye, A. Omojola, Drivers of deforestation and land-use change in southwest Nigeria, in: W. Leal Filho (Ed.), Handbook of Climate Change Resilience, Springer International Publishing, Cham, 2018, pp. 1–24, https://doi.org/10.1007/978-3-319-71025-9_139-1.

[97] P. Singh, O. Javeed, NDVI based assessment of land cover changes using remote sensing and GIS (A case study of srinagar district, Kashmir), Sust. Agric. Food Env. Res. 9 (2021), https://doi.org/10.7770/safer-V0N0-art2174.

[98] B. Khallef, R. Zennir, Forest cover change detection using normalized difference vegetation index in the oued bouhamdane watershed, Algeria - a case study, J. For. Sci. 69 (2023) 254–265, https://doi.org/10.17221/192/2022-JFS.

[99] MdR. Islam, MdN.I. Khan, MdZ. Khan, B. Roy, A three decade assessment of forest cover changes in Nijhum dwip national park using remote sensing and GIS, Environ. Chall. 4 (2021) 100162, https://doi.org/10.1016/j.envc.2021.100162.

[100] D. Luam Da Silva Panta, G. Alan De Sousa Soares, J. Stefany Da Silva Vila Nova, D. Dantas Moreira Gomes, Analysis of land cover and use through the soil-adjusted vegetation index (SAVI) in the context of environmental degradation in the municipality of lajedo/pernambuco, northeast, BRAZIL, IJSA 4 (2021), https://doi.org/10.56346/ijsa.v4i4.101.

[101] S. Pesaresi, A. Mancini, G. Quattrini, S. Casavecchia, Mapping mediterranean forest plant associations and habitats with functional principal component analysis using landsat 8 NDVI time series, Remote Sens. 12 (2020) 1132, https://doi.org/10.3390/rs12071132.

[102] P. Barreira González, V. González Cascón, J. Bosque Sendra, Detección de errores temáticos en el CORINE Land Cover a través del estudio de cambios: Comunidad de Madrid (2000-2006), Estud, Geogr. 73 (2012) 7–34, https://doi.org/10.3989/estgeogr.201201.